REFINED CHEMICAL COMPOSITION OF THE MURRAY FORMATION, GALE CRATER, MARS, AS MODELED WITH OBSERVATIONS BY THE ALPHA PARTICLE X-RAY SPECTROMETER. S.J. VanBommel[1], R. Gellert[1], J.A. Berger[2], E.D. Desouza[1], C.D. O'Connell-Cooper[3], L.M. Thompson[3], N.I. Boyd[1], [1]University of Guelph, Guelph ON, Canada, [2]University of Western Ontario, London ON, Canada, [3]University of New Brunswick, Fredericton NB, Canada.

Introduction: Compared to average Mars, the Murray formation[1] in Gale Crater is distinctly characterized by low MgO and CaO concentrations accompanied by enrichments in SiO_2, K_2O, and Ge, with an elevated Fe/Mn ratio. While *Curiosity*'s Alpha Particle X-ray Spectrometer[2] (APXS) analyses show this pattern is consistent over kilometers, chemical heterogeneities arise from intermixed dust, sulfates etc. in the APXS field of view.

We apply a least-squares mathematical deconvolution to a selection of APXS Murray targets to provide better constraints on the composition of what is characteristic of the Murray formation. By subtracting the contribution of likely additions with known composition (e.g. contaminating dust, $MgSO_4$, $CaSO_4$), this composition is a better representation of the Murray formation and will be referred to as "typical Murray". The model is not sensitive to whether the sulfates are in veins, nodules, or cements. Sulfates within the bulk rock (detrital or cements) have been observed in the Murray formation. These sulfates are potentially subtracted in the deconvolution but are important and discussed further in [3].

We then investigate modeling Murray target compositions as a mixture of thin dust, $MgSO_4$, $CaSO_4$, and derived typical Murray endmembers, to probe slight variations within the Murray formation along *Curiosity*'s traverse.

Method: At the heart of the analysis is a least-squares minimization routine analogous to existing APXS deconvolution algorithms[4]. VanBommel et al.[4] calculated the unknown composition for endmembers of a known relative contribution provided the number of APXS measurements exceeded the number of endmembers. Here, we calculate the unknown relative abundance of endmembers of known (or calculated) composition that best models APXS-measured concentrations.

The chemical composition of a number of endmembers, including dust, $MgSO_4$ and $CaSO_4$, as well as the APXS-measured composition of several targets, are input to the algorithm. The abundance of each endmember that minimizes the least-squares difference between the modeled and the APXS-measured composition is output as well as a goodness of fit (χ^2). Note, the least-squares fit may overestimate the amount of sulfur associated with $CaSO_4$ or $MgSO_4$ and remove sulfur potentially bound in other mineral phases not directly included in the modeled endmembers (i.e. jarosite). In addition to the abundance of each endmember, the script also iteratively searches for an additional endmember (and its abundance) that further improves the χ^2. This additional endmember represents the composition that is most representative of the "missing signal" from modeling the dataset with just the specified endmembers input. For example, with endmembers of dust and sulfates, the additional "missing signal" endmember would be most indicative of the dust- and sulfate-free composition native to all targets: typical dust- and sulfate-free Murray. Due to the iterative and convergent nature of the algorithm, uncertainties in the converged dust- and sulfate-free typical Murray composition correspond to the range observed over the lowest-χ^2 results.

The composition of the thin dust endmember was derived from a physics-based model. Using the dust composition from Berger et al.[5], we assume and calculate the contribution of a thin (5 μm) layer of dust. The sampling depth Z-dependence of the emitted characteristic X-rays results in the modeled thin dust composition that is similarly enriched in lower-Z elements as presented by Berger et al.[5]. Due to the nature of endmember modeling and deconvolution of target compositions, this is a better approximation of the contribution from a thin dust layer potentially overlaying targets than simply taking the optically thick dust or soil composition.

With the derived typical Murray composition, we model each individual Murray target as a mixture of thin dust, $MgSO_4$, $CaSO_4$ and typical Murray. The ratio of the measured composition to the modeled composition infers targets (or sets of targets/regions) along the traverse that are unique and are not simply a mixture of typical Murray plus dust and sulfates.

Results and Discussion: Figure 1 illustrates the derived composition for typical Murray (black, bold line) ratioed to average Mars. Noticeable differences are apparent when comparing to the direct Murray average (red dashed line). This captures the importance of considering the significant variation and subtle heterogeneities within the Murray formation when determining a characteristic composition. The range in compositions observed within the Murray formation scatters considerably around average Mars. However, as evident in Fig. 1, the signature of typical Murray (black, bold) is distinctly characterized by the low

MgO and CaO concentrations compared to average Mars. In addition, considering Ca-, Mg-sulfates and the potential contamination of a thin dust layer, typical Murray is significantly depleted in sulfur. The significant enrichments in K_2O, Zn, and Ge, compared to average Mars, are also evident in the derived typical Murray composition (Fig. 1). These enrichments are not as clear when looking at the overall range of concentrations across all Murray targets (shaded grey background).

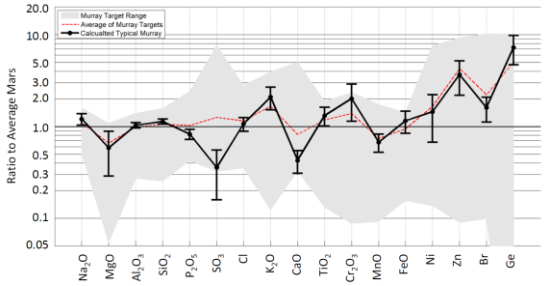

Figure 1: *Compositional range of APXS targets within the Murray formation (shaded, grey) and the corresponding average (red, dashed). Typical Murray (black, bold) calculated with dust and sulfate contribution removed.*

Figure 2 illustrates the ratio of measured to modeled concentrations of each target by sol (Mars days since landing, proxy for traverse). A ratio greater than unity indicates the measured concentration was higher than can be modeled by simply mixing dust, sulfates, and the previously derived typical Murray. This "enrichment" is interpreted as something extra that exists within the measured sample to give the increased concentration that the model cannot achieve. The most notable example of this is Buckskin, one of the high SiO_2 samples, interrogated from sol 1057-1091. The model is not only unable to produce the high-SiO_2 composition as a simple mixing, but also other elements, like K, Al, and Ti, deviate significantly, indicating a significant compositional change from typical Murray. Other examples of such systematic deviations are: the elevated Ni (and $MgSO_4$) of Morrison (sol ~775), the elevated Al_2O_3 of Mojave (sol ~800-900), and the gradually increasing Fe/Mn ratio (by decreasing Mn with near-constant FeO). One also sees the constant CaO, after the impact of $CaSO_4$ is removed, as well as the steady SiO_2, TiO_2, and FeO, aside from Buckskin. There also appears to be a downward trend in Mn and Zn along the traverse while there is an increase in Cl and Br (not plotted).

Conclusions: The encountered chemical homogeneity of the Murray formation, while a significant finding by itself with major implications for the geologic record at Gale, provides an opportunity to test existing algorithms in new ways. The derivation of typical Murray composition, absent apparent $CaSO_4$, $MgSO_4$, and dust, is important as it permits the potential to detect and quantify faint variations within the Murray formation as *Curiosity* continues its traverse.

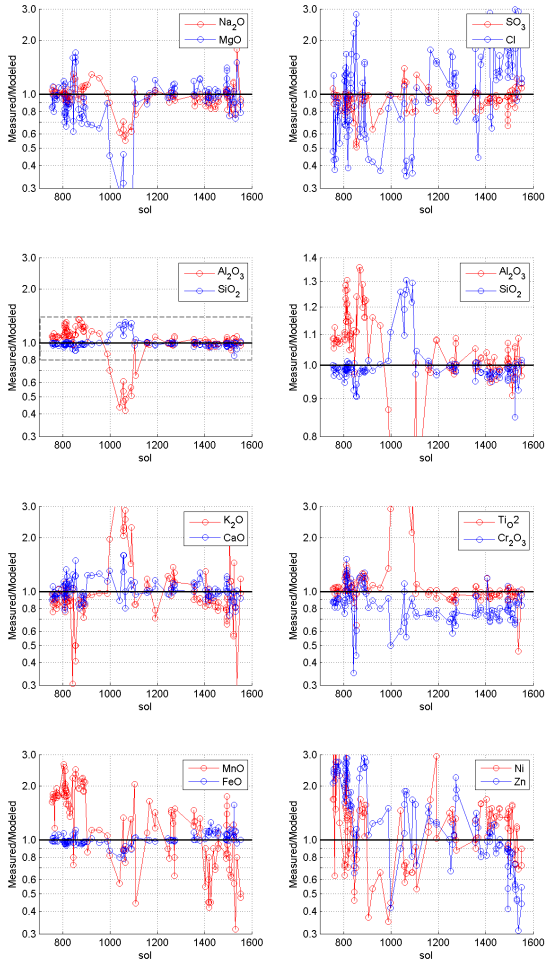

Figure 2: *Ratio of APXS-measured composition to model composition built from a least-squares mixture of thin dust, $MgSO_4$, $CaSO_4$, and derived typical Murray. A ratio greater than unity implies potential local enrichment (higher measured concentration than can be modeled by simply mixing dust, sulfates, and typical Murray).*

References: [1] Grotzinger et al. (2015) *Science*, 350(6257). [2] Gellert and Clark (2015) *Elements*, 11, 39-44. [3] Thompson et al. (this meeting). [4] VanBommel et al. (2016) *XRS*, 45(3), 155-161. [5] Berger et al. (2016) *GRL*, 43 67-75.

Acknowledgements: This work has been supported by the Canadian Space Agency (CSA) under contract 9F052-14-0592. The MSL APXS is financed and managed by the CSA with MacDonald Dettwiler and Associates as the primary contractor to build the instrument. Funding is provided by the CSA and NASA. Much appreciation goes to JPL for their support, dedication, and invaluable expertise.